Proceedings of the Seventh International Conference on
Railway Technology: Research, Development and Maintenance
Edited by: J. Pombo
Civil-Comp Conferences, Volume 15, Paper 17.13
Civil-Comp Press, Edinburgh, United Kingdom, 2026
ISSN: 2753-3239, doi: 10.4203/ccc.15.17.13


# Towards Predictive Railway Infrastructure Monitoring Using Axle Box Acceleration: A Case Study of the Otta Bridge

**C. Caspersen, M. Skjæveland, T. Ursin and A. Lau**

**IBM, NTNU, Trondheim, Norway**

## Abstract

This study investigates whether Axle Box Acceleration measurements from passenger trains in regular operaton can be used to identify changes in track and substructure conditions at the Otta Bridge. The motivation is based on the damage event in January 2025, where foundation movement affected the railway infrastructure.

The acceleration data are analysed within a common spatial framework by linking measurements to GPS positions. The study applies RMS, FFT, and wavelet analysis to examine local variations in vibration response around the bridge.

The results are used to assess whether changes in the acceleration signals can indicate track or substructure degradation. The findings aim to support more continuous and data-driven monitoring of railway infrastructure.

**Keywords:** axle box acceleration, railway monitoring, predictive maintenance, railway infrastructure, rail maintenance strategy, root mean square, track geometry

# 1 Introduction

In January 2025, train traffic on the Dovre Line in Norway was halted due to damage to the railway bridge over the Otta river, shown in Figure 1. High water levels and ice formation caused erosion around the southern abutment, leading to movement in the bridge foundation and displacement of the track shown in Figure 1 [15]. Such changes in the foundation and substructure can affect the dynamic response of both the bridge and adjacent track, for example through alterations in stiffness, damping, and load transfer. These effects may appear as changes in vibration levels and frequency content in acceleration measurements from passing trains, highlighting the need for more continuous and data driven monitoring of railway infrastructure.

The purpose of this study is to investigate whether Axle Box Acceleration (ABA) measurements from trains in regular service (Type 73 trains), together with track geometry data from the Roger 1000 measurement vehicle, can be used to detect such changes and potentially predict track and bridge displacement. The hypothesis is that indicators of developing damage may be present in the acceleration data prior to the event. Measurements from both systems are available before and after the incident, allowing for comparison and analysis. The study focuses on whether these data can be used for maintenance purposes and for early detection of track-related issues through frequency-based analysis.

The analysis is limited to lateral acceleration data to identify deviations, patterns, and potential sources of error. External factors such as temperature, weather conditions, and axle load are not included, as they are either unavailable or considered outside the scope of this study. Track geometry data from Roger 1000 are included to support the interpretation of the results.

Traditionally, railway track condition assessment relies on periodic inspections using dedicated measurement vehicles, which provide detailed but temporally limited data. By utilizing sensor data from trains in regular operation, it becomes possible to enable more continuous monitoring. Understanding how the frequency content of acceleration signals changes due to weakening in the track and substructure may contribute to earlier detection of deviations.

The study is relevant for stakeholders responsible for safe and efficient railway operation. Improved condition monitoring can support better maintenance decisions, reduce corrective interventions, and increase reliability in train traffic. By developing methods for systematic analysis of sensor data from operational trains, the study contributes to a more proactive and data-driven maintenance strategy, improving both the robustness and sustainability of the railway system.


Figure 1: Railway bridge over the Otta river with visible track alignment and inspection work following the 2025 damage event [16] (left). Km 296.788 along the Dovre Line [4] (right).

# 2 Method

## 2.1 Train and accelerometer information

Roger 1000 is a diesel powered railcar from 2001 equipped with two engines producing nearly 1000 horsepower. The train is 24 meters long and weighs 62 tonnes [12]. Approximately twice a year Roger 1000 measures track conditions including track geometry defects, lateral deviations, rail profiles, corrugation and wear in the rail surface, as well as acoustic measurements. Class 73A (Type 73) is an electric multiple unit consisting of four cars, three of which are powered. The trainsets were manufactured by ADtranz at Strømmen Værksted in Norway. Both trains are illustrated in Figure 2.


Figure 2: Picture of Roger 1000 (left) [5] and Type 73 train (right) [6].

ABA sensors are used to capture the dynamic interaction between the vehicle and the track. These accelerometers are typically mounted on or near the axle boxes, allowing them to measure vibrations transmitted from the wheel rail contact. The recorded signals contain information about track irregularities and potential defects in both the rail and the underlying structure [13].

In 2022, a national project started the project titled Measurement with Regular Trains in Traffic (MeTinT), supporting the installation of sensors on regular passenger trains, specifically the Type 73. The objective is to investigate whether onboard sensors can be used to monitor the condition of railway infrastructure. This approach has the potential to increase the monitoring frequency of both infrastructure and rolling stock without the need for specialized measurement equipment.

As part of this approach so were accelerometers installed on Type 73 trains as part of onboard monitoring systems used during normal operation. The sensors are mounted close to the wheel axles, providing measurements that are directly influenced by the wheel rail interaction. The sensor placement is designed to ensure consistent and repeatable measurements while minimizing noise from non track related sources. Since these trains operate under regular service conditions, the data reflect real traffic loads, speeds, and environmental influences. This enables continuous monitoring of track conditions over time and provides a large volume of data for analysis.

In contrast, the Roger 1000 measurement vehicle is equipped with a more specialized sensor setup, including high-precision accelerometers mounted on the axle boxes. The sensor configuration is optimized for measurement accuracy and repeatability, often under controlled operating conditions. This allows for detailed inspection of track geometry and dynamic response, making the data well suited for identifying specific defects and validating observations from operational trains [14]. However, in this study, only the track geometry data from Roger 1000 are utilized, as acceleration data are not available from before the incident.

Differences in sensor placement, measurement quality, and operating conditions between the Type 73 trains and the Roger 1000 vehicle must be considered when comparing the datasets. While the Roger 1000 provides high-resolution track geometry measurements, the Type 73 trains provide continuous, real-world acceleration data. Together, they provide a complementary basis for analyzing track condition and detecting potential degradation.

## 2.2 Data description

### 2.2.1 Roger1000 track geometry data

The Roger1000 system is specifically designed to capture variations in the track and is therefore well suited for obtaining detailed measurements of track geometry. In this study, only track geometry data from Roger1000 are used to support the analysis.

Track geometry data for different measurement days were provided by a supervisor at Bane NOR. The datasets cover sections from station to station, where the endpoints vary between the measurement days, but all include the area around Otta Bridge. The two datasets used in the analysis are:

- Vinstra – Dombås (approximately 76 km), 17 June 2024
- Tretten – Dombås (approximately 129 km), 16 June 2025

The data include coordinates and train speed in addition to the track geometry measurements. The geometry data consist of parameters such as longitudinal level, which describes vertical irregularities relative to a reference position, and alignment, which represents lateral deviations of the track. Other parameters include twist, cant, curve, and track gauge. In this study, the main focus is on longitudinal level and alignment, as these are considered the most relevant for the analysis.

#### 2.2.2 73 train

The dataset from the Type 73 train consists of two main file types: NI-data and Cdc-Data. NI-data contains high-frequency (1400 Hz) measurements from accelerometers in both vertical and horizontal directions, as well as microphone data stored in TDMS files. The data span a three-year period and are organized into one folder per day and one file per 10 minute interval, including periods when the train is not in operation. The files are accessed through multiple cloud platforms depending on the time period. Cdc-Data consists of daily CSV files with GPS coordinates (latitude and longitude) and train speed sampled at 1 kHz, which are used to link the NI-data to positions along the track. Although Cdc-Data also includes accelerometer measurements, these are less accurate and are therefore not used further. Since the two datasets have different sampling frequencies, they are synchronized using linear interpolation to ensure accurate alignment of acceleration data with position.

### 2.3 Analysis method

#### 2.3.1 Basic vibration and interpolation

Vibration measurements from accelerometers are recorded as discrete time series with a constant sampling frequency. For a signal $x(t)$ sampled with frequency $f_s$, the time of each measurement point can be expressed as

$$t_i = t_0 + \frac{i}{f_s} \tag{1}$$

where $t_0$ is the start time and $i$ is the sample index. Such a representation forms the basis for further signal processing [1, Chapter 2].

Interpolation is used to estimate intermediate values between known data points. One method is linear interpolation, where two points are connected by a straight line representing a first-order interpolation polynomial [2, Chap. 18]. For the points $(x_0, f(x_0))$ and $(x_1, f(x_1))$, an intermediate value can be calculated as

$$f_1(x) = f(x_0) + \frac{f(x_1) - f(x_0)}{x_1 - x_0}(x - x_0). \tag{2}$$

The method provides a good approximation when the points are closely spaced, as a continuous function can be well approximated by a straight line [2, Chap. 18]. In this thesis, linear interpolation is used to assign a GPS position to each accelerometer sample, so that the vibration data can be analyzed within a common temporal and spatial reference.

When analyzing vibration levels, RMS (root mean square) is often used as a measure of the signal's effective amplitude. For a discrete signal defined over $N$ measurement points, RMS is given by

$$\text{RMS} = \sqrt{\frac{1}{N}\sum_{i=1}^{N} x_i^2}.$$

The RMS value represents the mean square value of the signal and is directly related to the signal's energy level. Moving RMS is often used to describe local variations in vibration levels over time or space [3]. The method therefore provides a measure of how vibration intensity develops along the track or during a passage.

### 2.3.2 Fast Fourier Transform

To examine the frequency content of the vibration signal, the Fast Fourier Transform (FFT) is applied to a selected signal segment around the point of interest [8]. In this paper the segment is extracted within a small spatial window around the chosen track position. This is so that the frequency response can be analyzed locally.

Before computing the FFT, the mean value of the signal segment is removed to eliminate any constant offset. A Hanning window is then applied to reduce spectral leakage and improve the representation of the dominant frequency components [7]. Since the accelerometer signal is real-valued, only the non-negative part of the frequency spectrum is used.

The FFT is used here to compare the local frequency content of different train passages at the same location. This makes it possible to identify dominant frequency components and assess whether the vibration response changes between measurements. In the present analysis the FFT is therefore used as a tool to study how the spectral characteristics of the acceleration signal vary around the selected point. This within the chosen window and under the applied filtering settings.

### 2.3.3 Wavelet

In addition to frequency-domain analysis, wavelet analysis is used to examine how the frequency content of the vibration signal evolves over time [9]. This is particularly useful for non-stationary signals where the frequency characteristics change within a short time interval. An example of this is a train passage over a specific location.

Similar to the FFT analysis, a signal segment is extracted within a small spatial window around the selected point. The mean value is removed prior to analysis in order to avoid bias from constant offsets. A continuous wavelet transform (CWT) is then applied using a complex Morlet wavelet (cmor), which provides a good balance between time and frequency resolution [10].

The wavelet transform produces a time frequency representation of the signal where the energy content can be visualized as a function of both time and frequency [11]. This makes it possible to identify transient events and localized changes in vibration behavior that may not be clearly visible in the FFT.

In this study the wavelet analysis is used to complement the FFT by providing insight into how the vibration response develops as the train passes the selected point. This allows for a more detailed interpretation of the dynamic behavior. Particularly in cases where short duration effects or localized anomalies are of interest.

## 2.4 Data Processing Workflow

Figure 3 illustrates the overall structure of the data processing workflow, divided into two branches corresponding to the two data sources and their respective processing pipelines.

The workflow begins with a search through GPS data (CSV files) to identify train passages within a defined radius around a selected point, which here is the southern abutment of Otta Bridge. The candidate matches are manually verified before further use in the analysis.

### 2.4.1 Train-based accelreation data branch (73-train)

The target coordinates and analysis window are defined, after which each TDMS file is processed sequentially. Acceleration data are matched to the corresponding GPS file based on timestamp. The travel direction of each passage is determined to ensure consistent comparison between passages.

GPS positions are then interpolated to match the resolution of the acceleration data, assigning a precise track location to each measurement sample. Cumulative distance along the track is computed, followed by quality control to verify that the passage provides sufficient spatial coverage within the analysis window.

The acceleration signal is filtered and a moving RMS is calculated to characterize vibration levels. After processing, the passages are grouped and plotted as a function of track position. Local spectral analysis (FFT) and time–frequency analysis (wavelet) are performed within a narrow window around the selected point.

### 2.4.2 Track geometry branch (Roger 1000)

Following the initial GPS search and match verification, the track geometry data are loaded and validated. Cumulative distance along the track is computed, and data within the same coordinate window as defined for the train-based acceleration data are extracted.

Travel direction is standardized to ensure consistent orientation across measurement days. Relevant geometry parameters are then selected and plotted as a function of track position, enabling direct spatial comparison with the train-based results.

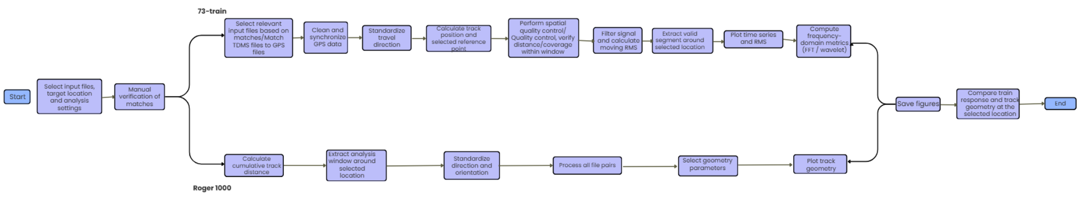


Figure 3: Flowchart for the code.

# 3 Results

The results are presented for a selected point at the transition between the bridge and the southern abutment at Otta Bridge (km 296.788), where both acceleration data and track geometry are visualized. The coordinates of the point are (61.76828, 9.53835), as shown in Figure 1. The acceleration data are obtained from the Type 73 train, while the track geometry data is based on measurements from the Roger 1000 system.

## 3.1 Roger 1000

The vertical and horizontal deviation of the track for selected days before and after the event is shown in Figure 4. The selected days are 17 June 2024 (before the event) and 16 June 2025 (after the event).

A clear dip can be observed around the selected point in both the alignment and longitudinal level graph. For the alignment (AL), the deviation in 2025 reaches approximately above 5-6 mm, whereas in 2024 it is around 2-3 mm. The longitudinal level (LL) graph also shows a clear dip at the same location, corresponding to a vertical irregularity in the track. However, unlike the alignment, the longitudinal level

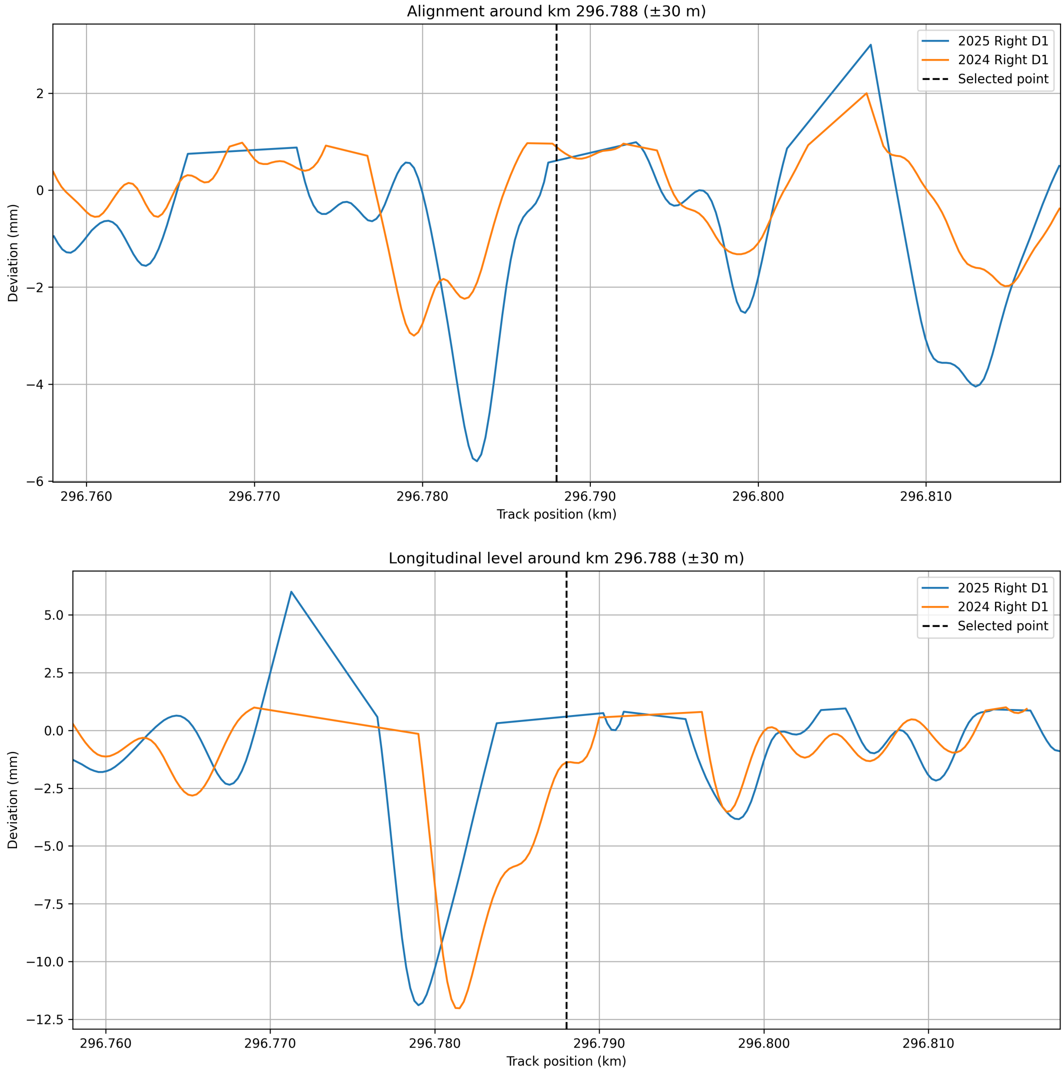


Figure 4: Alignment (AL, top) and longitudinal level (LL, bottom) around the selected track section. The figures are based on Roger 1000 track geometry measurements.

does not show a clear increase or trend in displacement between the two years.

Both deviations occur at approximately the same location, corresponding to the transition between the bridge and the adjacent track. A spatial offset of about 10 m is observed between the datasets. This offset may be related to limitations in positioning accuracy, as the recorded position does not necessarily coincide with the exact physical point on the track where the measurement is taken. Consequently, both datasets may be subject to small spatial offsets relative to the selected reference point.

Although there is no direct requirement for a correlation between vertical and lateral deviations, their co-location suggests that they may originate from the same underlying mechanism. A possible explanation is differential settlement, where the ballast gradually compresses over time while the bridge structure remains relatively stable. In addition, a minor displacement of the bridge structure itself may contribute to the observed behaviour.

## 3.2 73 train

The results from the Type 73 train measurements are presented in Figures 5-6. The analysis focuses on a selected point near the Otta bridge, where time series, RMS, FFT, and wavelet analyses are used to investigate changes in vibration behaviour before and after the incident. The selected days represent the closest available ABA measurements before and after the event. To ensure a consistent comparison, only data from northbound runs are included, as the response may not be symmetric with respect to direction. The selected days are 2 January 2025 (before the event) and 3 June 2025 (after the event). The results are interpreted with consideration of operational conditions such as train speed and potential spatial offsets between datasets.

The acceleration time series and corresponding RMS values shown to the left in Figure 5, calculated using a moving window of 50 ms, indicate increased vibration levels near the selected point in the June 2025 data, after the incident. This observation is somewhat unexpected, as a reduction in vibration levels might be anticipated following maintenance or stabilization measures. The selected point was identified visually and may therefore not exactly coincide with the true location of the transition. Compared to the offset observed in Figure 4, the time series and RMS results appear to be shifted in the opposite direction by approximately 2 m. This may be explained by the same factors as previously discussed. In addition, GPS accuracy may be reduced in valley environments such as Gudbrandsdalen, where the Otta bridge is located, due to less favourable satellite geometry. This offset is assumed to be systematic (fixed offset), likely related to differences in sensor position, GPS accuracy, and the definition of the reference point. No correction has been applied in this study due to time limitation.

It should be noted that the measurements are obtained under real traffic conditions. The train speed varies slightly around 60 km/h between the selected passages, as indicated in Figure 5. Although the variation is relatively small, speed differences may influence both the amplitude and frequency content of the measured vibrations and should be considered when comparing the datasets.

Variations in axle load, speed, and environmental conditions may therefore influence the results, and differences between the two measurement days cannot be explained solely by changes in track condition.

The track geometry data from Roger1000 show both vertical and lateral deviations at the selected location, indicating that the track irregularity has components in both directions. This suggests that the train–track interaction at this point is influenced by a combined geometric effect. Although only horizontal acceleration data are analysed in this study, the observed response is likely affected by this combined irregularity. Possible explanations include movement at the abutment or gradual changes in the ballast

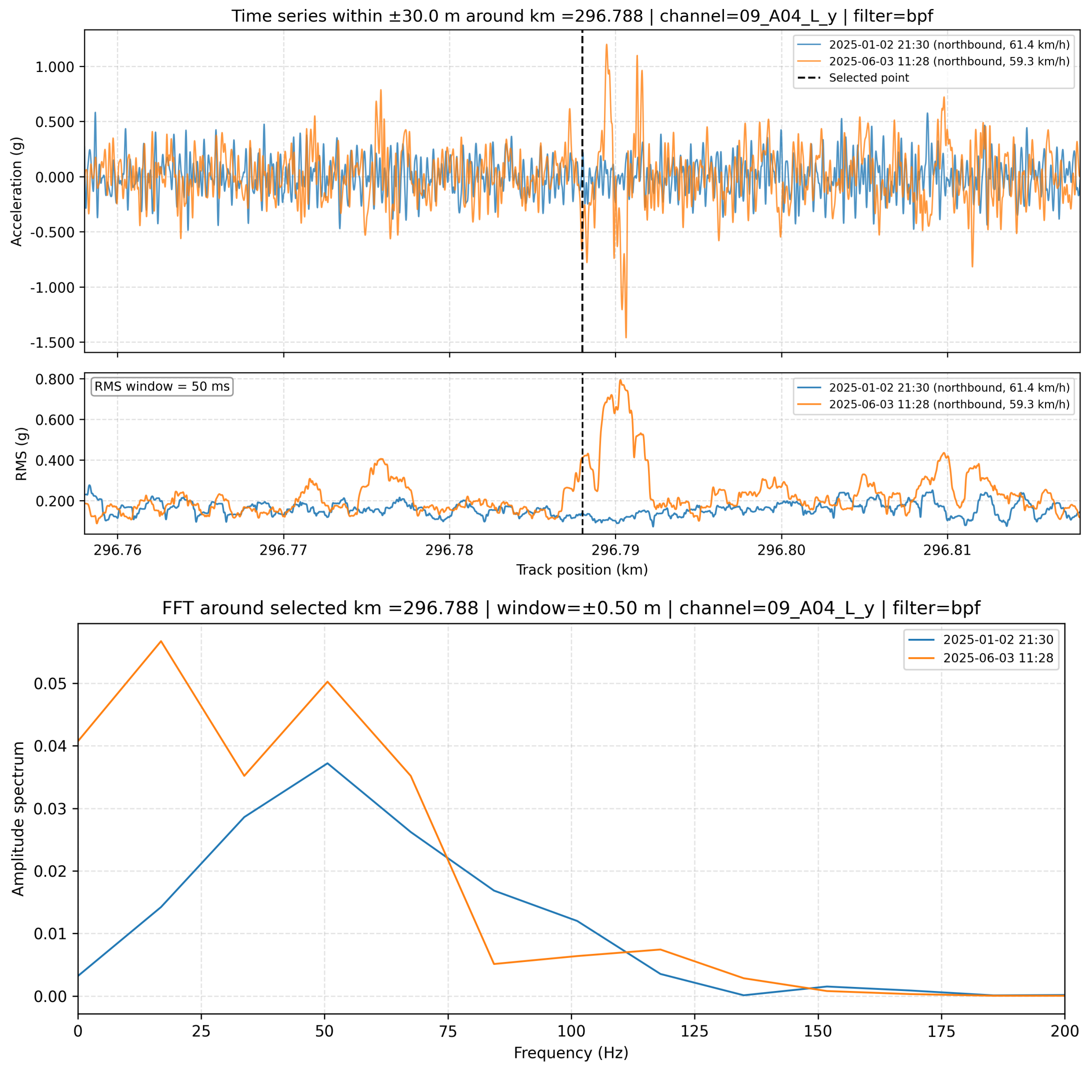


Figure 5: Acceleration time series and RMS (left) and corresponding frequency spectrum obtained using FFT (right) for the Type 73 train around the selected point.

condition due to repeated loading. Insufficient ballast compaction or redistribution of ballast material may reduce track stiffness and increase the dynamic response under train loading, which can contribute to higher vibration levels and altered frequency content.

The FFT analysis is based on a spatial window of ±0.5 m around the selected point, with a band-pass filter allowing frequencies between 0.1 Hz and 100 Hz to pass. This range is chosen to capture the response from local track irregularities, considering the observed displacement and the train speed. For a train speed of approximately 60km/h, this frequency range corresponds to wavelengths from about 0.17 m to 167 m, indicating that both short- and long-wavelength track irregularities are included in the analysis.

A difference in frequency content is observed between the two measurement days. The time series and RMS indicate increased overall vibration levels after the event, which is also reflected in the FFT as higher amplitudes in certain frequency components. This indicates that the change is not only related to the overall magnitude of the vibrations, but also to how the vibration energy is distributed across frequencies. To investigate how these frequencies vary along the track, a wavelet analysis is performed and shown in Figure 6.

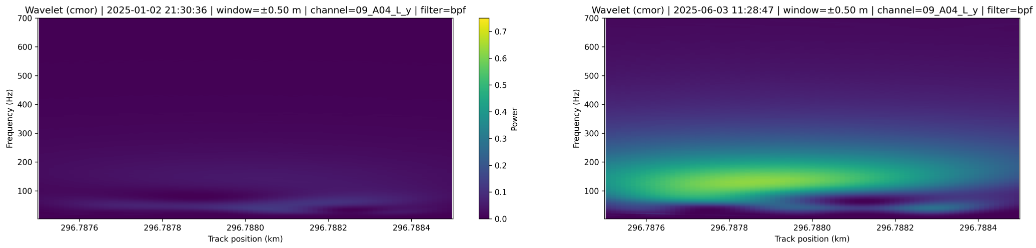


Figure 6: Wavelet analysis for two different measurement days for the Type 73 train around the selected point. The plots illustrate the time–frequency distribution of the vibration signal.

The wavelet analysis provides a time–frequency representation of the signal, making it possible to identify where along the track these frequency components occur.

The results show localized changes in energy within the relevant frequency range at the transition zone, indicating a change in vibration behaviour at this location.

The maximum wavelet power within the 0.1–100 Hz range at the selected point is higher after the event, increasing from 0.125 to 0.625, indicating a substantial increase in vibration energy. The wavelet results indicate that the vibration energy is mainly concentrated below 100 Hz before the event, while a clear increase is observed in the range of approximately 80–150 Hz after the event. This suggests a shift in the frequency content and a change in vibration behaviour at the transition zone.

It should be noted that the available measurements may not capture the most critical period immediately before the event. The track condition could therefore have been more severe closer to the time of the incident, followed by an improvement after maintenance and a gradual development towards the conditions observed in the later measurements.

# 4 Concluding remarks

This study has investigated whether Axle Box Acceleration measurements from Type 73 trains, combined with track geometry data from Roger 1000, can be used to detect changes in track and substructure conditions at Otta Bridge.

The track geometry results show a localized deviation in both alignment and longitudinal level at the transition between the bridge and the adjacent track. The co-location of these deviations suggests a common underlying mechanism, likely related to differential settlement between the track and the bridge structure or insufficient ballast compaction.

Based on the limited dataset used in this study, the results do not show a clear indication that the track condition was worse prior to the maintenance measures following the event. Although changes in vibration behaviour are observed between the two measurement days, the results do not follow the expected trend of reduced vibration levels after maintenance.

A possible explanation is that the measurements do not capture the most critical period immediately before the event. It is therefore likely that the track condition may have been more severe closer to the time of the incident, followed by an improvement after maintenance, and a subsequent development towards the conditions observed in the later measurements.

Consequently, the findings should be interpreted with caution. While the results demonstrate that acceleration-based measurements are sensitive to changes in track behaviour, the available data are insufficient to establish a clear relationship between the measured response and the progression of damage over time.

Further work should focus on extending the analysis with additional data and refining the methods in the context of the master's thesis, with the aim of improving the reliability of such approaches for continuous railway monitoring.

## Acknowledgements

This work is funded by the Norwegian Railway Directorate (Jernbanedirektoratet). The authors would like to thank KONNEKT for support in the implementation of this work.

# References

[1] A.V. Oppenheim, R.W. Schafer, J.R. Buck, Discrete-Time Signal Processing, Prentice Hall, Upper Saddle River, NJ, 1999, 2nd edition.

[2] S.C. Chapra, R.P. Canale, Numerical Methods for Engineers, McGraw-Hill Education, New York, 2015, 7th edition.

[3] D.I. Crecraft, S. Gergely, Signals and signal processing, in: D.I. Crecraft, S. Gergely (Eds.), Analog Electronics, Butterworth-Heinemann, Oxford, 2002, pp. 13–71.

[4] Bane NOR, Banekart, available online: https://banekart.banenor.no/kart/, accessed 16 November 2025.

[5] Bane NOR, Nå er det lenge siden vi har postet om Roger 1000, italieneren som kjenner den norske jernbanen bedre enn noen andre, Instagram post, 2022, available online: https://www.instagram.com/p/CiAe7LaKi_b/?hl=en&img_index=1.html, accessed 21 November 2025.

[6] Norske tog, Class 73 - A series, available online: https://www.norsketog.no/en/trains/motor-vehicles/type-73-serie-a, accessed 14 October 2025.
[7] MathWorks, Hann window, Signal Processing Toolbox Documentation, available online: https://www.mathworks.com/help/signal/ref/hann.html, accessed 7 April 2026.
[8] MathWorks, Fast Fourier Transform (FFT), available online: https://www.mathworks.com/discovery/fft.html, accessed 7 April 2026.
[9] N.P. Subramaniyam, Time-Frequency Analysis and Wavelets, Sapien Labs, available online: https://sapienlabs.org/time-frequency-analysis-and-wavelets/, accessed 7 April 2026.
[10] W.C. Jin et al., A Study on the Continuous and Discrete Wavelet Pattern Analysis of EM Signal Measurements, Sensors, 26(5), 1507, MDPI, 2026, available online: https://www.mdpi.com/1424-8220/26/5/1507, accessed 7 April 2026.
[11] K. Wirsing, Time Frequency Analysis of Wavelet and Fourier Transform, in: S. Mohammady (Ed.), Wavelet Theory, IntechOpen, 2020, available online: https://www.intechopen.com/chapters/74096, accessed 7 April 2026.
[12] Bane NOR, Roger gjør togreisen tryggere, Bane NOR, 2022, available online: https://www.banenor.no/nyheter-og-aktuelt/nyheter/2022/roger-jakter-pa-vindskjeve-spor/, accessed 7 April 2026.
[13] I. Bravo, U. Alvarado, J. Nieto, P. Ciáurriz, On-board accelerometers in railway track condition monitoring: A systematic review, Transportation Research Interdisciplinary Perspectives, 33, 101572, 2025, available online: https://www.sciencedirect.com/science/article/pii/S2590198225002519, accessed 7 April 2026.
[14] CEMIT AS, Instrumentation report, CEMIT AS, 2024, internal technical report.
[15] Stine Bækkelien, Even Lusæter, Bjørnar Morønning, Arne Sørenes, Bane Nor visste om dårleg tryggleik på Otta bru – no er brua skuva på og Dovrebanen stengd, NRK, 2025, available online: https://www.nrk.no/innlandet/bane-nor-visste-om-darleg-tryggleik-pa-otta-bru.-na-er-brua-skuva-pa-og-dovrebanen-stengd-1.17217393, accessed 7 April 2026.
[16] T. Karlsen, M. G. Solberg, Bare midtpilarene ble sikret da brua sto i fare for å kollapse – landkarene forble urørt, Teknisk Ukeblad, 30 Jan. 2025, available online: https://www.tu.no/artikler/bare-midtpilarene-ble-sikret-da-brua-sto-i-fare-for-a-kollapse-landkarene-forble-urort-br/555211, accessed 7 April 2026.